

Field-Oriented Control for Squirrel-Cage Induction Generators in Pump as Turbines Applications

Samuel Amaro
samuel.amaro@tecnico.ulisboa.pt

Instituto Superior Técnico, Lisboa, Portugal

January 2021

Abstract

Pumps operating as turbines (PATs) are a way of improving efficiency in water systems. In these systems, pressure-reducing valves are typically used to regulate the pressure for the water consumers, by dissipating the excess of energy. The PAT is a better alternative to these valves, allowing the recovery of this excess of energy. This solution is especially useful in isolated areas without access to the electrical grid. In this work it is intended to develop a field-oriented control algorithm that allows control of electrical and mechanical quantities of the generation system and maximizes its efficiency. This algorithm was first developed to control the induction machine speed in stand-alone operation and then changed to control the generator's electromagnetic torque and its shaft's mechanical power. Finally, coupling the PAT to the induction generator, several tests were performed to validate the control algorithms. Since the subject of interest is off-grid operation, it is intended to replace the capacitor banks used in previous works to excite the machine for a three-phase inverter fed by a battery. The maximum efficiency of the generating unit obtained in simulation was 49,8 % under control conditions.

Keywords: Energy efficiency, Field-Oriented Control, Induction Generator, Loss Minimization, Off-grid Pump as Turbine

1. Introduction

With the increasing need to avoid depleting natural resources, water supply systems have shown the potential to be used as electrical energy recovery systems. According to [1], it is possible to recover up to 188 MW h/year for 910000 m³/year of water that is being wasted in Valencia, Spain. In addition to the waste of water, the high required water pressures may also lead to water leakages and pipes damage. Currently, a solution for that consists of installing pressure-reducing valves, reducing the water pressure and leakages. However, these pressure-reducing valves do not allow the energy recovery. By changing these valves for hydraulic machines such as PATs (pumps as turbines), one can, at the same time, prevent such damage and recover electrical energy by coupling it to a generator. This kind of energy recovery, complemented by energy storage units, presents a well-known technology and offers a low-cost solution, easy installation, and maintenance [2].

The study's actual interest is the PAT's and generator's off-grid operation for low power applications in rural and remote areas. Capelo [3], but also Williams et al. [4] have identified the induc-

tion generator as the most appropriate electrical machine to take into account for energy recovery in water distribution systems. In these situations, factors such as reliability, cost-effectiveness, robustness, and maintenance costs have the same importance as performance and efficiency.

When the electrical grid is present, it supplies the necessary reactive power for the machine excitation. Its absence means that the induction generator has to be excited by some other source. In previous works, the behavior of the PAT-SEIG system was analyzed for a stand-alone application, with capacitor bank to provide the SEIG excitation. These works focused on: a) the impact of the change of SEIG electric parameters on the overall system's efficiency; b) the electro-hydraulic transients on the system due to sudden changes and c) on the behavior of series-connected PAT-SEIG systems.

The work done in [5] has established the required range of capacitance values to excite the generator as a function of its load. This work considered that all generator parameters were constant for every operating point. The maximum efficiency of the generating unit obtained was 26 % for a speed of 1200 rpm and a water flow of 4.7 l s⁻¹.

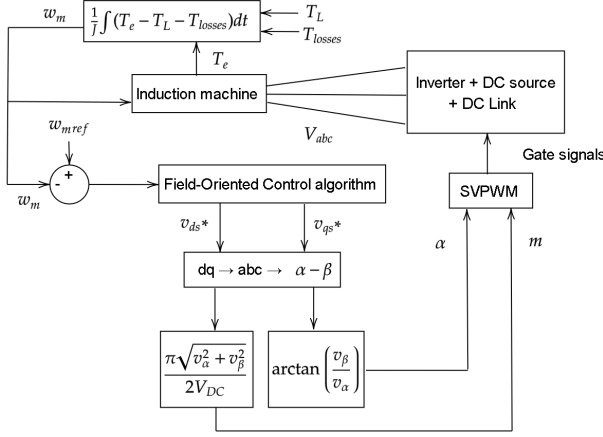


Figure 2: Field-Oriented control scheme for speed control with inverter.

$$\lambda_{qr} = 0 \quad (3)$$

$$\theta_s = \int w_s dt = \int \left(w_m \frac{p}{2} - \frac{R_r i_{qs}}{L_r i_{ds}} \right) dt \quad (4)$$

$$i_{ds}^* = \frac{\lambda_{dr}^*}{L_m} \quad (5)$$

$$i_{qs}^* = \frac{2}{3} \frac{2}{p} \frac{L_r}{L_m} \frac{T_e^*}{\lambda_{dr}^*} \quad (6)$$

where p is the number of pole pairs of the machine, w_s the electrical stator angular speed, w_m the the mechanical speed of rotation (in rad s^{-1}), R_r the rotor windings resistance and L_r the total rotor inductance. λ_{qr} is the leakage flux of the rotor windings in the quadrature axis, θ_s is the electrical angle between stator and the frame direct axis and L_m the mutual inductance between stator and rotor.

2.2. Stand-alone operation: electromagnetic torque and mechanical power control

Electromagnetic torque T_e and mechanical power P_{mec} are related as follows

$$P_{mec} = T_e w_m \quad (7)$$

In the tests performed for this types of control, speed w_m was assumed to be constant and equal to the machine's rated speed of 910 rpm ($95,3 \text{ rad s}^{-1}$), so only a single control variable is used (torque or mechanical power). With a constant speed, Eq. (7) shows that both types of control must be equivalent, i.e., one can know torque when imposing a mechanical power reference value and vice-versa.

To control electromagnetic torque, instead of using a reference speed and a PI controller to generate

the reference torque as shown in Figure 1, one just has to impose the torque value. To control mechanical power, one can use the same algorithm used for speed control, but use mechanical power as input instead of speed. If the power at a given moment is less than the reference power, the difference will be positive, which will increase torque. As the speed of rotation is constant, this translates into an increase of mechanical power, as can be concluded through Eq. (7).

To perform the simulations, it will be assumed that rotor flux is equal to the rated flux (1,04 Wb).

2.3. Loss minimization in steady-state

Operating the machine at rated flux will be far from optimal in a variety of situations. Most of the time, the machine will operate in partial-load regime and run below its rated efficiency. To bypass this problem, the field-generating current i_{ds} and consequently the generated magnetic field needs to be reduced to an optimal level, allowing the same torque to be obtained with a lower stator current, resulting in lower ohmic and iron losses in the machine. In this section, the objective is to use a method to minimize the induction machine ohmic losses in steady-state operation.

From [8], the optimal flux, i.e., the flux that minimizes ohmic losses in steady-state, depends on torque and machine parameters and is given by

$$\lambda_{dr,opt}^* = \sqrt{\frac{2}{3} \frac{T_e^*}{p} \left(\frac{R_s L_r^2 + R_r L_m^2}{R_s} \right)^{\frac{1}{4}}} \quad (8)$$

2.4. Generating unit - inclusion of the PAT

When coupling the PAT to the generator there are new inputs to the system: water pressure P and flow rate Q . Head drop H (m.w.c) is defined as

$$H = \frac{P}{\rho g} \quad (9)$$

where ρ is fluid density (kg m^{-3}) and g is the gravitational acceleration (m s^{-2}). Pressure P is in Pa. Flow rate Q ($\text{m}^3 \text{ s}^{-1}$) can be calculated through the PAT Q-H curves, that were obtained experimentally in [3]. This curves were interpolated by a second-order polynomial since it is a typical type of curve for a PAT

$$H = \alpha^2 A + \alpha B Q + C Q^2, \quad (10)$$

which can be written as

$$Q = \frac{-\alpha B \pm \sqrt{(\alpha B)^2 - 4C(\alpha^2 A - H)}}{2C}, \quad (11)$$

$\alpha = \frac{N_r}{N_{ref}}$. The coefficients A, B and C and the reference speed N_{ref} were obtained with experimental data and are: $A = 3,6644; B = 94,45; C =$

314560 and $N_{ref} = 1050$ rpm. To complete the model, hydraulic power, hydraulic torque and mechanical torque have to be computed. The hydraulic power transferred to the shaft is given by

$$P_{hyd} = QP = \rho g QH \quad (12)$$

Hydraulic torque can be calculated as

$$T_{hyd} = \frac{P_{hyd}}{\omega_m}, \quad \omega_m = N_r \frac{2\pi}{60} \quad (13)$$

The output mechanical torque on the pump shaft is given by

$$T_{mecPAT} = T_{hyd}\eta_{PAT} \quad (14)$$

The mechanical coupling equation of the system is

$$J \frac{d\omega_m}{dt} = T_{mecPAT} + T_e - T_{losses} \quad (15)$$

Note that T_{mecPAT} is a positive value and T_e is a negative value because the induction machine is operating in generator mode. In steady-state, the PAT model must return the electromagnetic torque produced by the induction machine apart from losses.

The generating unit efficiencies are as follows

$$\eta_{PAT} = \frac{P_{mec}}{P_{hyd}}, \quad \eta_{gen} = \frac{P_s}{P_{mec}}, \quad \eta_{global} = \eta_{PAT}\eta_{gen} \quad (16)$$

2.5. Inclusion of the magnetizing resistance in the machine model

The machine model and the field-oriented control algorithm have to be rearranged when including the magnetizing resistance. Both deductions can be found in [9], so only the final results will be presented. The magnetizing resistance will be calculated based on experimental data obtained previously in [6]. Interpolating the data resulted in

$$\frac{R_m}{f} = -2.5635 \left(\frac{E}{f}\right)^2 + 20.7288 \left(\frac{E}{f}\right) - 7.845 \quad (17)$$

To obtain the value of R_m the last step is to multiply the ratio R_m/f by the frequency f , given by

$$f = \frac{\omega_s}{2\pi}, \quad \omega_s = \int \theta_s dt \quad (18)$$

When including the magnetizing resistance, optimal flux expression according to [8] becomes

$$\lambda_{dr,opt}^* = \sqrt{\frac{2 T_e^*}{3 p}} \left(\frac{R_s L_r^2 + R_r L_m^2}{R_s L_r^2 + L_m^4 \frac{p^2 \omega_m^2}{R_m}} \right)^{\frac{1}{4}} \quad (19)$$

3. Results

3.1. Stand-alone operation: speed control

Simulations were made for the machine rated speed of 910 rpm at no load (no external torque T_L applied). After tuning the PI controllers proportional and integral gains (named P and I respectively), the final result obtained is shown in Figure 3. It can be seen that convergence speed is satisfactory and there are no oscillations when reference speed is achieved.

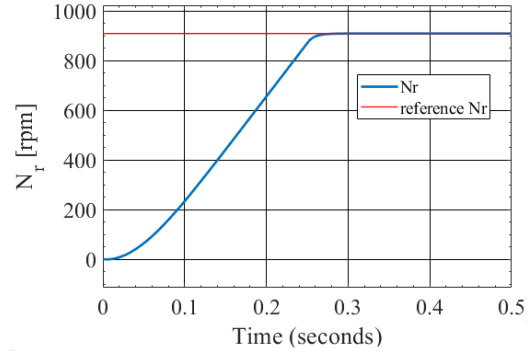


Figure 3: Ideal case of speed control: motor speed for P = 10, I = 1000 (torque controller), P = 1000, I = 10000 (current controllers).

3.2. Stand-alone operation: electromagnetic torque and mechanical power control

This tests were performed for the machine rated values of torque ($-5, 8$ N m) and mechanical power (-550 W) assuming a constant speed of 910 rpm. This values are negative since the machine is operating in generator mode. The results obtained are present in Figures 4 and 6. As in speed control, no oscillations are present and convergence speed is even better.

Efficiency of the generator is shown in Figure 5 for the entire range of operation of reference values of torque. For very low torques, it can be seen that the machine is operating as motor, i.e, consuming active power. In motor mode, the machine's efficiency is not defined as in Eq.(16) and is instead given by P_{mec}/P_s . That is the reason why efficiency is shown to be zero for very low torques in Figure 5. There are two reasons why the machine may be operating in the motor mode for these values: the fact that the stator resistance is very high, which will result in high dissipated power due to the magnetization current, and the fact that the rotor flux is kept constant and equal to its nominal value for the entire range of operation. Low torques mean that the machine is operating in a partial load regime. Therefore, using rated flux to generate the magnetizing current i_{ds} will cause the machine's efficiency not to be the best possible.

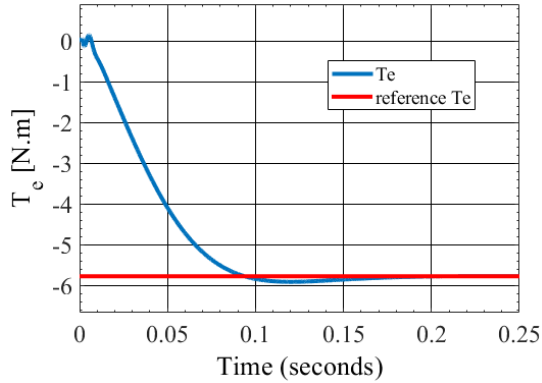


Figure 4: Ideal torque control: torque for $P = 100$, $I = 100000$ (current controllers).

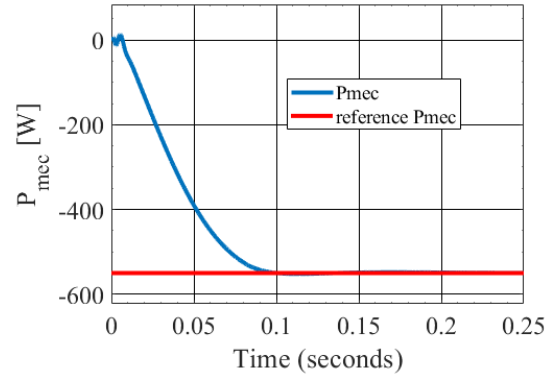


Figure 6: Ideal mechanical power control: mechanical power for $P = 10$, $I = 1000$ (torque controller) and $P = 100$, $I = 100000$ (current controllers).

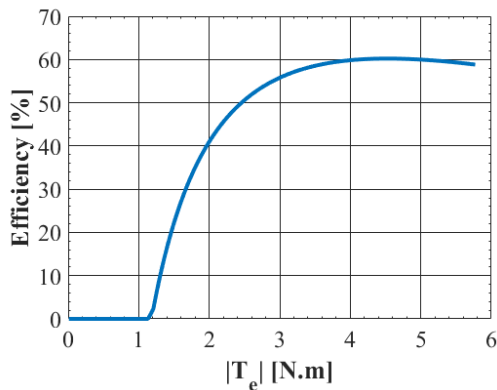


Figure 5: Ideal torque control: generator efficiency as function of the absolute value of electromagnetic torque.

3.3. Stand-alone operation: loss minimization method results

To verify the loss optimization, tests were made for torque control. As seen, torque and mechanical power control are equivalent for a constant speed. The tests consist of simulating the machine behaviour for a variety of torque reference values and computing its efficiency, assuming that the machine is running at its rated speed (910 rpm), but using optimal flux (Eq. 8). Figure 7 shows the efficiency of the generator under this assumptions. Results present in Figure 5 were included for comparison.

The results obtained for the operation at optimal flux are substantially better. Efficiency is now closer to 60% throughout the entire range of reference values. The improvement of efficiency for lower torque values is notorious because now the machine is always operating in generator mode, meaning that it is supplying active power on the stator. For values closer to the nominal point of operation, one can conclude that the results are the same for operation at rated flux and optimal flux. Indeed, for

higher values of torque, the optimal flux is approximately equal to the rated flux because it is proportional to the square root of the torque, as seen in Eq. (8). Figure 8 shows the evolution of optimal flux for different values of torque.

Figure 9 confirms what has been concluded until this point. For low values of torque and mechanical power, losses are smaller than when using rated flux. For operation points near the nominal point, the usage of optimal flux or rated flux will produce the same results simply because the closer one gets to the nominal point, the closer optimal flux and rated flux become.

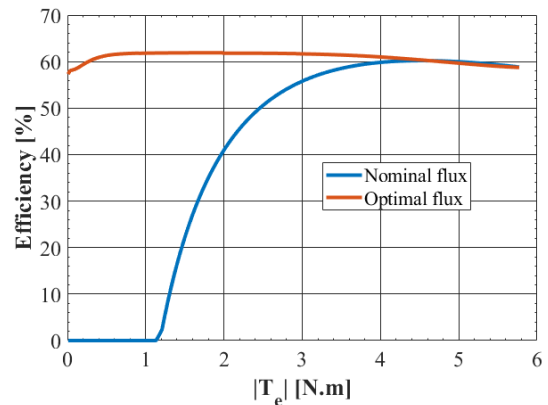


Figure 7: Induction machine efficiency as function of the module of electromagnetic torque for operation at rated speed (910 rpm).

3.4. Generating unit: speed control

The PAT is now coupled to the induction machine. The objective is to understand how a change in water pressure P affects the system. Simulations were performed for three turbine water pressures: 80%, 100% (or nominal pressure, equal to 72100 Pa), and 120%. Figure 10 shows the generating unit global

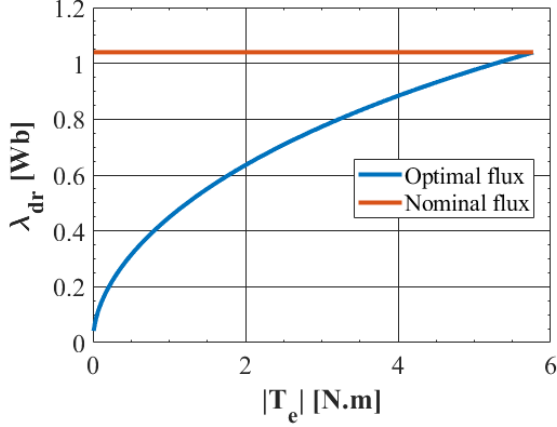


Figure 8: Rotor flux as function of the module of electromagnetic torque for operation at rated speed (910 rpm).

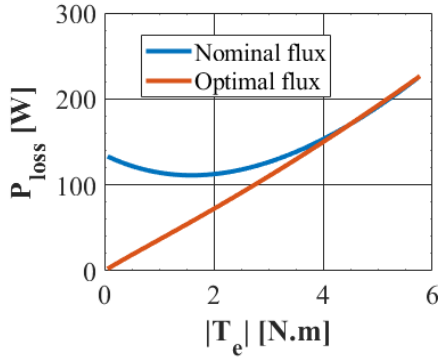


Figure 9: Power losses as function of the module of the electromagnetic torque for operation at rated speed (910 rpm).

efficiency obtained in these tests as a function of the group speed when the steady-state operation was reached. For a pressure of 80 % of the nominal one, maximum efficiency was 47 % for a speed of 1365 rpm. For the nominal pressure (72100 Pa), maximum efficiency was 49,7 % for a speed of 1505 rpm, and for 120 % of the nominal pressure, maximum efficiency was 49,8 % for a speed of 1715 rpm.

Figure 11 shows the evolution of active power and mechanical power as function of speed. As expected, the higher the pressure, the higher the maximum delivered power will be. For a given pressure, there is a peak for power and then it starts decreasing. This has to do with the flow rate behaviour: it decreases as speed increases (Eq. (11)). Therefore, increasing speed will result in lower hydraulic power, since hydraulic power is proportional to flow rate (Eq. (12)), but not in lower efficiencies as seen in Figure 10. That is why as speed increases, mechanical power and, therefore, active power increase

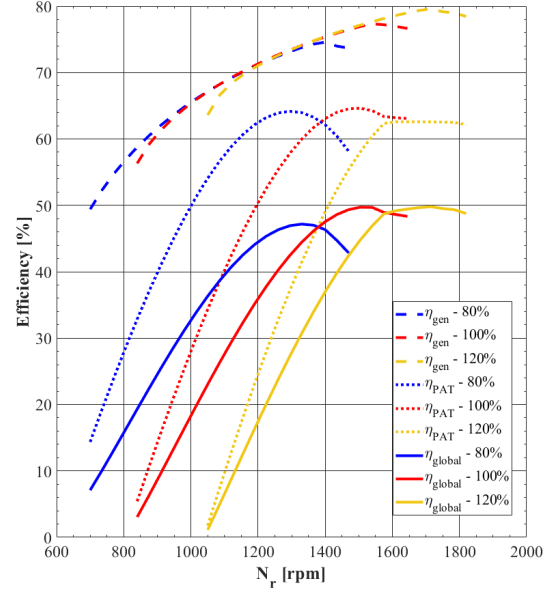


Figure 10: Speed control of the generating unit: efficiencies of the generator, PAT and global for operation at different water pressures.

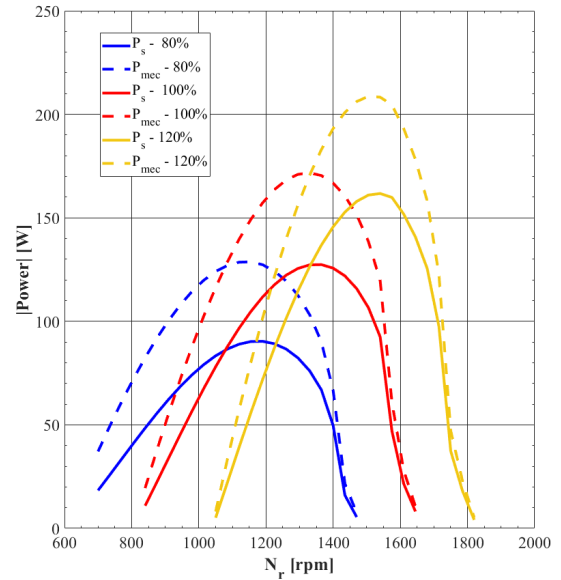


Figure 11: Speed control of the generating unit: stator active power (solid lines) and mechanical power (dashed lines) in absolute value as function of speed for operation at different water pressures.

in the first stage (efficiencies increase at a faster rate than the rate of decrease of hydraulic power), but then start to decrease as efficiency stabilizes.

3.5. Generating unit: electromagnetic torque and mechanical power control

Figure 12 shows the evolution of active power delivered by the generator stator when performing mechanical power control. As seen, it can be concluded that mechanical power control allows one to supply the load with constant active power, even though water pressure changes. This makes sense since one controls mechanical power and the generator efficiency has variations smaller than 3% for the entire range of operation (see Figure 13).

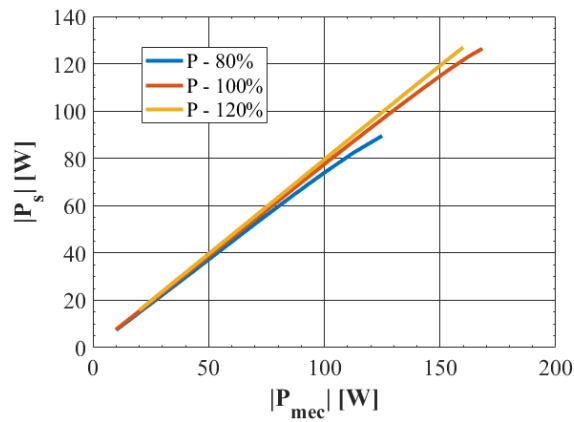


Figure 12: Mechanical power control of the generating unit: stator active power in absolute value as function of the absolute value of mechanical power for operation at different water pressures.

Figure 14 illustrates active power and mechanical power when performing torque control. As shown, one can no longer supply the load with constant active power regardless of pressure, which was possible when controlling mechanical power. Depending on the pressure, the same torque value will result in a different mechanical power on the shaft (different speed) and consequently a different active power on the generator stator.

The shape of the power curves present in Figure 11 show that mechanical power and torque control are not the most reliable way of controlling the system. For instance, by observing Figure 12 one sees that, for operation at 80% of rated water, the maximum controllable mechanical power was -120 W (blue line), whereas by looking at Figure 11 the maximum mechanical power obtained pressure was -135 W (blue dashed line). In mechanical power control, it was observed that if the reference value kept increasing above -120 W the system started to become unstable and could no longer be controlled because the closer one gets to the maximum possi-

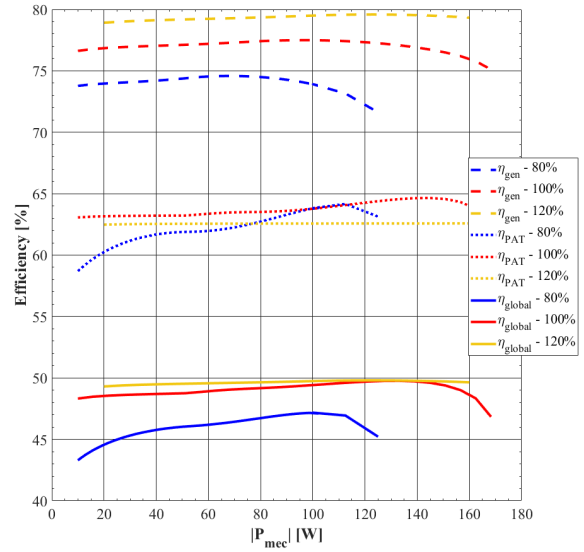


Figure 13: Mechanical power control of the generating unit: efficiencies of the generator, PAT and global for operation at different water pressures.

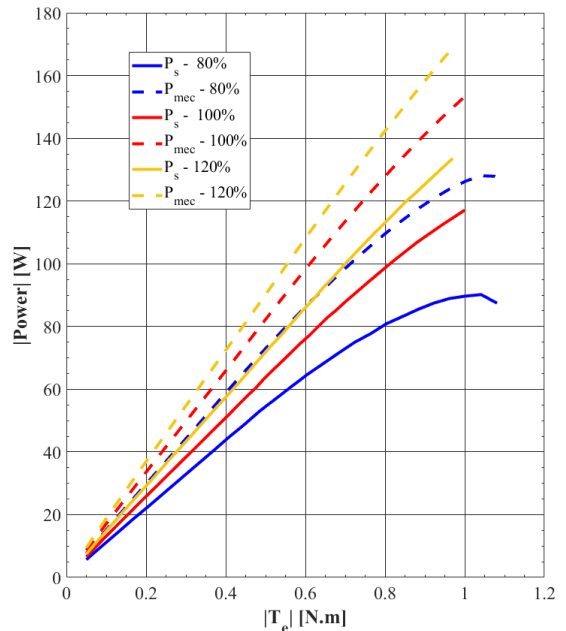


Figure 14: Torque control of the generating unit: stator active power (solid lines) and mechanical power (dashed lines) as function of absolute value of electromagnetic torque for operation at different water pressures.

ble value, the closer the two possible points of operation are, i.e., their corresponding speeds are less far apart, as illustrated in Figure 11. In addition to this, the nominal point of operation of the generator (5,8 N m / 550 W) was never reached, since mechanical power on the group shaft was never higher than 200 – 300W.

The most important conclusion regarding mechanical power control is that it allows one to supply the load with constant active power, even though water pressure changes. In torque control, this is not possible, as shown in Figure 14. In terms of efficiency, this two types of control will put the system operating at pretty much constant efficiency for the entire range of reference values, as shown in Figures 13 and 15.

When performing speed control, the PAT will have very different operation points, so its efficiency (and consequently global efficiency) will assume a wider range of values than in mechanical power and torque control, as shown in Figure 10. The generator efficiency has been optimized by applying the loss minimization method to reduce rotor flux, so it does not have much influence in the generating unit global efficiency regardless of the control type used.

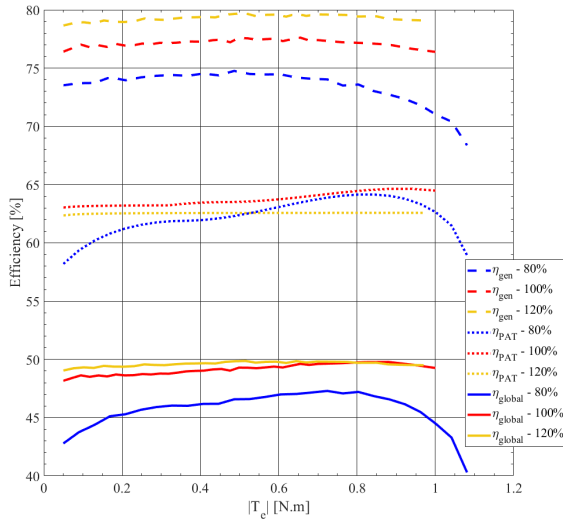


Figure 15: Torque control of the generating unit: efficiencies of the generator, PAT and global for operation at different water pressures.

3.6. Inclusion of the magnetizing resistance R_m

Figure 16 shows the generator efficiency in stand-alone operation, assuming a constant speed of rotation equal to 910 rpm as done in section 3.2. Recall that, with a constant speed, torque and mechanical power controls are equivalent. Results from Figure 5 are included for comparison. The maximum

efficiency obtained now was 48 % for an electromagnetic torque of -4 N m and a mechanical power of -384 W, whereas before this value was 60,2 %, showing a decrease of 20 % when using optimal flux. Nominal flux proved to be an extremely poor choice, since the machine cannot operate in generator mode for almost the entire range of reference values.

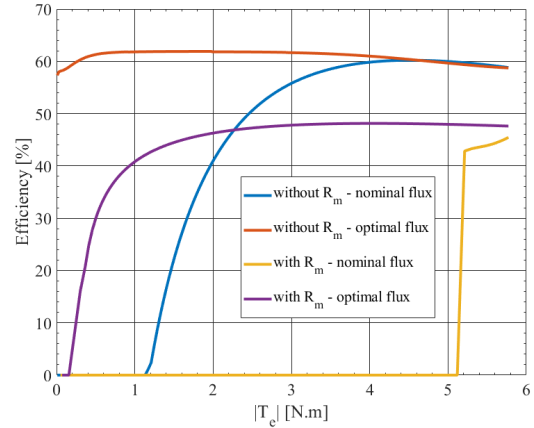


Figure 16: Ideal torque control: induction machine efficiency as function of absolute value of torque - comparison between results with and without magnetizing resistance for stand-alone operation.

Figure 17 shows global efficiency of the generating unit when performing speed control. Results from Figure 10 were included for comparison. The influence of R_m is high because the study was done for a low power induction machine. This influence becomes smaller for higher power machines.

Table 2 contains the differences between the top efficiencies obtained for both scenarios.

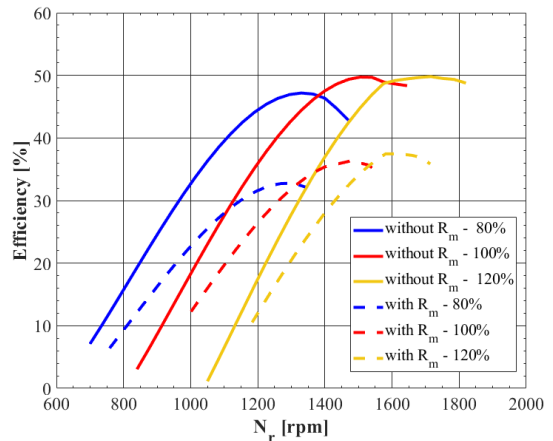


Figure 17: Speed control of the generating unit: comparison between global efficiencies obtained with and without iron losses.

Table 2: Top efficiencies obtained for both scenarios - with and without iron losses - and respective deviation when performing speed control of the generating unit.

Scenario	Top eff. without R_m [%]	Top eff. with R_m [%]	Difference [%]
P = 80%	47,2	32,8	30,5
P = 100%	49,7	36,4	26,8
P = 120%	49,8	37,5	24,7

4. Conclusions

As proposed, the field-oriented control algorithm was developed and tested for both the stand-alone generator operation and coupled to the PAT in steady-state regime. For the stand-alone generator operation, the control algorithm was initially designed for speed control and was then changed to allow electromagnetic torque and mechanical power control.

For these simulations, it was concluded that the generator efficiency was especially low in the partial-load regime, as the rated flux was imposed. Following these results, a method for optimizing the machine flux in steady-state operation was applied. It was seen that optimal flux, which is the one that minimizes losses, is a function of electromagnetic torque. When the machine is operating with optimal flux, the results showed a very significant improvement in the partial-load regime, with efficiency being nearly constant and approximately equal to 60 % for all points of operation of the machine at rated speed (910 rpm).

After this, the PAT was coupled to the generator with the field-oriented control algorithm and the loss minimization method. Further tests were performed to evaluate the generating unit behavior under control conditions. Speed control results were most revealing. They showed that the machine will have different operating points in terms of speed but will be supplying the load on the generator stator with the same active power. This means that a single control variable is not enough to impose the operating system point when performing either electromagnetic torque or mechanical power control. Besides, when trying to impose torque and mechanical power values close to the maximum obtained for speed control, the system started to become unstable. As one gets closer to those maximum values, the two possible operating points get nearer, meaning that they are very similar, so the system cannot know the desired operating point. Fortunately, it operated at higher global efficiency points. However, since these points have higher corresponding speeds (see Figure 10), it may not be of interest for the system to operate in this region.

In the end, the magnetizing resistance was included in the induction machine model to evaluate stand-alone operation efficiency and global ef-

iciency when coupled to the PAT. The results showed that efficiency decreased around 20% in stand-alone operation and 25 – 30% coupled to the PAT when iron losses were considered.

At last, it is worth mentioning that no control and/or optimization of the PAT hydraulic variables has been done. Besides, the pump as a turbine being used so far in the studies is a low power PAT. As seen, the generator’s nominal point of operation was never reached under any control method, so a higher power PAT may be suitable. These are pertinent topics to be studied in the future.

References

- [1] Pérez-Sánchez M, Sánchez-Romero F, Ramos H, López-Jiménez P. "Modeling irrigation networks for the quantification of potential energy recovering: a case study". *Water* 8:1–26/2016. <http://dx.doi.org/10.3390/w8060234>.
- [2] de Oliveira e Silva G, Hendrick P. Pumped hydro energy storage in buildings. *Appl Energy* 2016;179:1242–50. doi: <https://doi.org/10.1016/j.apenergy.2016.07.046>
- [3] B. Capelo. Energy Recovery in Water Distribution Systems by a Pump Running as Turbine (PAT) – Grid Isolated Case. Master thesis, Instituto Superior Técnico, May 2017.
- [4] A. A. Williams, N. P. Smith, C. Bird, and M. Howard. Pumps as turbines and induction motors as generators for energy recovery in water supply systems. *Water and Environment Journal*, 12(3): 175–178, 1998. doi: <https://doi.org/10.1111/j.1747-6593.1998.tb00169.x>
- [5] B. Capelo, M. Pérez-Sánchez, J. F. Fernandes, H. M. Ramos, P. A. López-Jiménez, and P. J. Branco. Electrical behaviour of the pump working as turbine in off grid operation. *Applied Energy*, 208(September):302–311, 2017. <https://doi.org/10.1016/j.apenergy.2017.10.039>.
- [6] J. F. P. Fernandes, M. Pérez-Sánchez, F. F. Silva, P. A. López-Jiménez, H. M. Ramos, and P. J. C. Branco. Optimal energy efficiency of isolated PAT systems by SEIG excitation tuning. *Energy Conversion and Management*, 183(January):391–405, 2019. <https://doi.org/10.1016/j.enconman.2019.01.016>.
- [7] M. Pagaimo, Pumps as turbines (PATs): Series and parallel connections. Master thesis, Instituto Superior Técnico, November 2019.
- [8] A. Dötlinger, R. Kennel, J. Stumper Loss Minimization of Induction Machines in Dynamic

Operation *IEEE Transactions on Energy Conversion*, 28 (September): 726 - 735, 2013. doi: <https://doi.org/10.1109/TEC.2013.2262048>

- [9] S. Amaro, Field Oriented Control for Squirrel-Cage Induction Generators in Pump as Turbines Application. Master thesis, Instituto Superior Técnico, December 2020.
- [10] Khoury. G, Ghosn R., Khatounian F., Fadel M., Tientcheu M. Including Core Losses in Induction Motors Dynamic Model. 2016 3rd International Conference on Renewable Energies for Developing Countries, Zouk Mosbeh, Lebanon. doi: <https://doi.org/10.1109/REDEC.2016.7577556>
- [11] Rossi M, Righetti M, Renzi M. Pump-as-turbine for energy recovery applications: the case study of an aqueduct. *Energy Procedia* 2016;101:1207–14. <https://doi.org/10.1016/j.egypro.2016.11.163>
- [12] Carravetta A, Derakhshan S, Ramos HM. *Pumps as Turbines Fundamentals and Applications*. Springer International Publishing; 2018. <https://doi.org/10.1007/978-3-319-67507-7>.
- [13] T. H. Phuong, MATLAB/Simulink Implementation and Analysis of Three Pulse-Width-Modulation (PWM) Techniques. Master thesis, Boise State University, May 2012.
- [14] S. D. Fitzgerald, A.E., Kingsley, Charles Jr., Umas. *Electric machinery*, volume 319. 2003. ISBN 0073660094. doi: 10.1016/0016-0032(85)90014-6.